ASSESSMENT OF A CHAMBERLESS ACTIVE HLFC SYSTEM FOR THE VERTICAL TAIL PLANE OF A MID-RANGE TRANSPORT AIRCRAFT

K.S.G. Krishnan, O. Bertram
German Aerospace Center (DLR), Lilienthalplatz 7, 38108 Braunschweig

Abstract

The objective of this paper is to analyze the system aspects for installation of an active hybrid laminar flow control system with a chamberless suction nose on the leading edge of the vertical tail plane of a mid-range transport aircraft. The inputs from various disciplines which are important from systems perspective are extracted, and the interfaces between various disciplines are drawn. A study is conducted to assess the proposed systems architectures, and a trade-off analysis is subsequently performed.

1. INTRODUCTION

Reducing the environmental impact of aviation is increasingly becoming an important priority for the aircraft designer in the 21st century [1]. As the aviation industry is an important contributor of noise and emissions of carbon dioxide (CO_2), much research is performed to create more environmentally sustainable aircraft. These priorities are reflected e.g. in the ambitious goals of ACARE's Vision 2020 and Flightpath 2050.

One means to reduce fuel consumption and hence CO_2 emissions in the cruise phase is the drag reduction obtainable by keeping the airflow laminar over the aircraft surfaces such as wings, horizontal tail plane (HTP), vertical tail plane (VTP) etc. In a laminar flow, the fluid layers slide smoothly over each other in a streamlined fashion, whereas in a turbulent flow, the fluid exhibits erratic motion [2]. From boundary layer theory we know that in the flow region close to the surface, viscous forces (skin friction) are dominant while at sufficient distance from the surface the flow is practically inviscid. In a laminar boundary layer, the velocity gradient ($\partial u/\partial y$) and hence the shear stress (τ), which represents the skin friction, are smaller than in a turbulent boundary layer, as shown in fig. 1. Here y is the distance from the wall scaled by the boundary layer thickness δ, u is the velocity scaled by the velocity outside the boundary layer U, and μ is the dynamic viscosity.

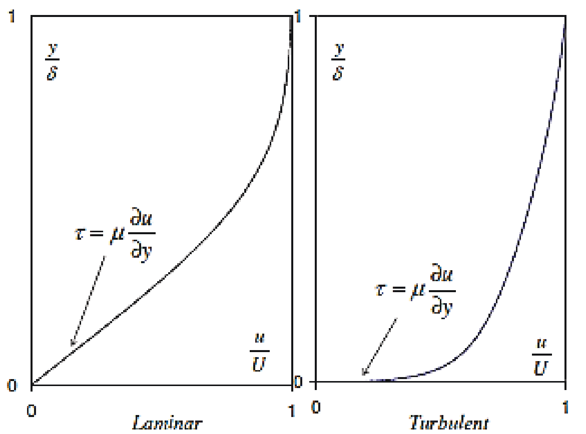

FIG 1. **Laminar and turbulent boundary layer velocity profile [1]**

Hence, the skin friction drag in a laminar boundary layer is far less compared to a turbulent one, rendering laminar flow the preference for aircraft wings, tail-planes and engine nacelles. However, while the boundary layers start laminar, they transition to turbulence after an intial streamwise distance, so that on the above surfaces the airflow is predominantly turbulent under normal operating conditions for conventional aircraft.

The laminar-to-turbulent transition is triggered by instability mechanisms such as Tollmien-Schlichting instability, crossflow instability and attachment line transition [2, 3]. Various possible flow laminarization techniques to counter the instabilities are shown in Fig. 2; the red lines mark the suction areas where a part of the boundary layer is extracted.

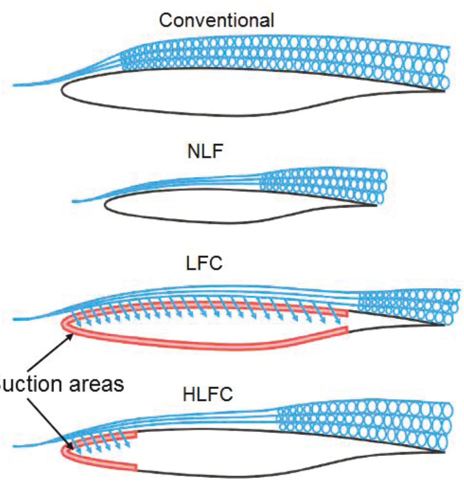

FIG 2. **Schematic comparison of NLF, LFC and HLFC – image [4]**

The NLF (natural laminar flow (airfoil shaping)) is suitable for wings with sweep angles up to 23° and Mach numbers till 0.75 [5], beyond which crossflow instability and attachment line transition become dominant and cannot be controlled by shaping the airfoil alone [6]. The LFC (laminar flow control (suction)) is not suitable because of complexity, high power consumption and space constraints [7].

For high-speed aircraft with large wing sweep, applying hybrid laminar flow control (HLFC) is a promising way to suppress these instabilities and to delay the transition.

The HLFC combines suction in the leading edge with a re-shaping of the airfoil to extend laminarization. It is basically a combination of LFC and NLF techniques. In an HLFC system, a small amount of air is sucked in at the leading edge of the surfaces. By doing that, instability mechanisms which usually trigger the transition from laminar to turbulent flow are delayed to higher chord percentages resulting in a greater laminar flow area with resulting less drag and fuel consumption.

This paper deals with the preliminary design trade-off study of a chamberless HLFC concept applied to the vertical tail plane (VTP) of a mid-range transport aircraft. Section 2 describes the various HLFC concepts and TuLam project, in section 3 the system assessment method is explained. Section 4 explains the performed architectures trade-off study.

2. HLFC CONCEPTS AND TULAM PROJECT

The HLFC for reducing aircraft skin friction drag in cruise conditions has been under research since the 1970's. Various concepts have been proposed and researched in the past decades. A brief summary of the different concepts is described below.

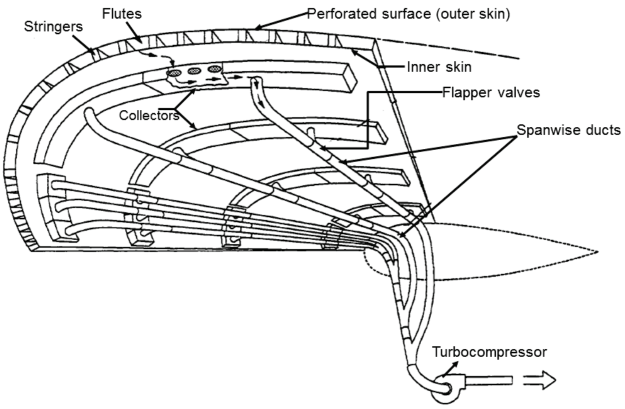

FIG 3. Suction system concept used in Boeing 757 flight test [8]

In the late 80's and early 90's, NASA / Boeing proposed and analyzed a suction system concept shown in Fig. 3, which was studied experimentally in flight tests conducted during the years 1987 – 1991 under the Boeing 757 flight test program. This concept consisted of a perforated surface, collector ducts and spanwise ducts to transfer the air from the collector to the transfer duct with the help of a turbocompressor, and an exhaust to expel the compressed air.

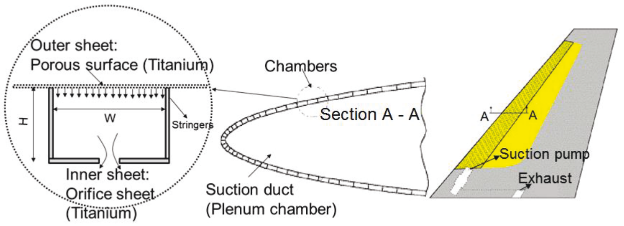

FIG 4. ALTTA Suction system concept [9]

In the EU, another variation has been proposed in the late 90's known as the ALTTA (Application of hybrid Laminar Technology to Transport Aircraft) concept [9] shown in Fig. 4. This concept consisted of a perforated surface, a double chamber, a plenum chamber and an exhaust. The double chamber had an outer micro-perforated sheet and an inner orifice sheet connected to the plenum, and consisted of different chambers separated by the stringers.

TuLam (Toughen up Laminar Technology) was a DLR internal research project from February 2014 to September 2017. It was the successor of the DLR internal research project LamAiR (Laminar Aircraft Research). The goal of TuLam was to increase the Technology Readiness Level of the laminarization technology and to further simplify the suction system needed for the HLFC technique.

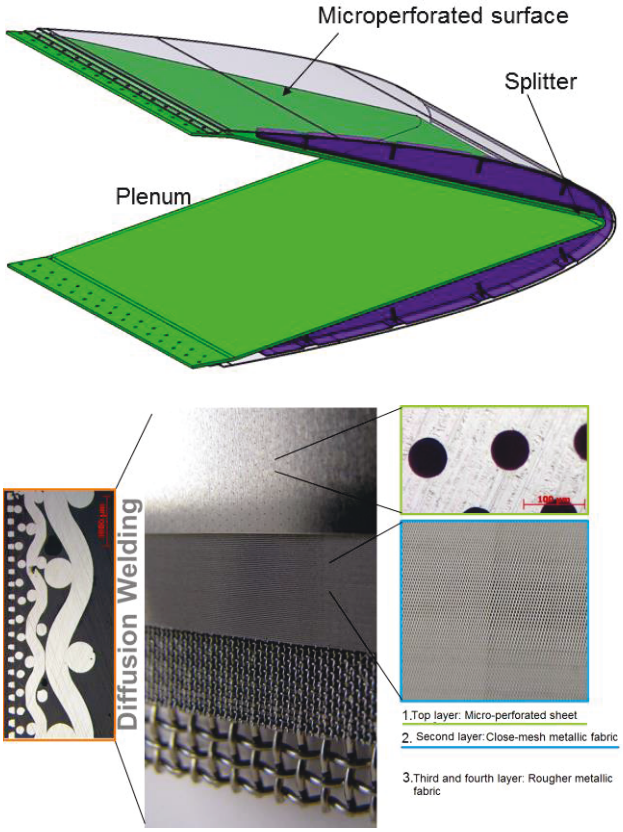

FIG 5. Chamberless HLFC suction nose concept, project TuLam

TuLam dealt with the investigation of an active HLFC system for the vertical tail plane (VTP) of a mid-range transport aircraft. The concept of a chamberless suction nose installed at the leading edge was initially proposed in LamAiR and further developed in TuLam (see fig. 5) including the assessment of the whole HLFC system for the vertical tail plane.

This concept considered a perforated surface, chamberless suction, a splitter section which is connected to the leading edge using the ribs and used as plenum chamber and an exhaust. The V-shaped splitter section is provided to counter bird strike effects [10].

3. SYSTEM ASSESSMENT METHOD

Besides the aerodynamic, structural and manufacturing analyses, also system aspects have to be considered in order to minimize system weight, power consumption as well as complexity and thus maximize the benefits of integrating yet another system into the aircraft. The various inputs from other disciplines to the systems are summarized in Fig. 6.

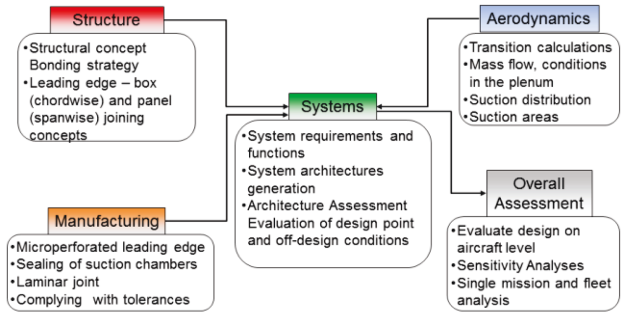

FIG 6. Inputs to systems and generated outputs [2]

The aerodynamics discipline provides the various pressures (static, surface and plenum pressures) and the mass flow rate for the design point conditions, as shown in Fig. 7. Here the design point is at FL310 and with a total mass flow of 0.474 kg/s.

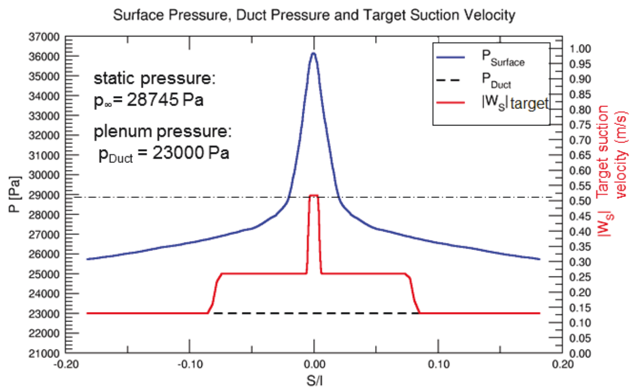

FIG 7. Design pressures and suction velocity distributions plotted against surface coordinates (S/l)

The structures discipline provides inputs regarding the geometry of the suction system. With these values as inputs, it is possible to assess different architectures. The important parameters for selecting optimal architectures in the preliminary design phase are suction power requirement and the resultant increase in fuel consumption as well as overall system mass added to the aircraft due to the HLFC installation. The subsequent subsections provide the method to estimate the power requirements, SFC and the additional system mass.

3.1. Suction power estimation

One of the main system requirements for the HLFC system is to produce suction in the leading edge of the VTP. This can be achieved by means of an active system using a compressor connected to the plenum chamber. In section 4.1, various system architectures are generated with compressors in different configurations, for performing system assessment. It is important to calculate the suction power requirements, and hence the power off-takes (POT) in order to compare the various architectures. Fig. 8 explains the method used for calculation of suction power.

The pressure drop for the chamberless concept mainly occurs in the pathway from the plenum to the transfer duct, in the transfer duct and in the exhaust duct. The pressure in the plenum stays constant. However, to transfer air from the plenum chamber to the compressor, there is contraction in area and hence there is pressure loss due to contraction [11] as given by Eqn. 1.

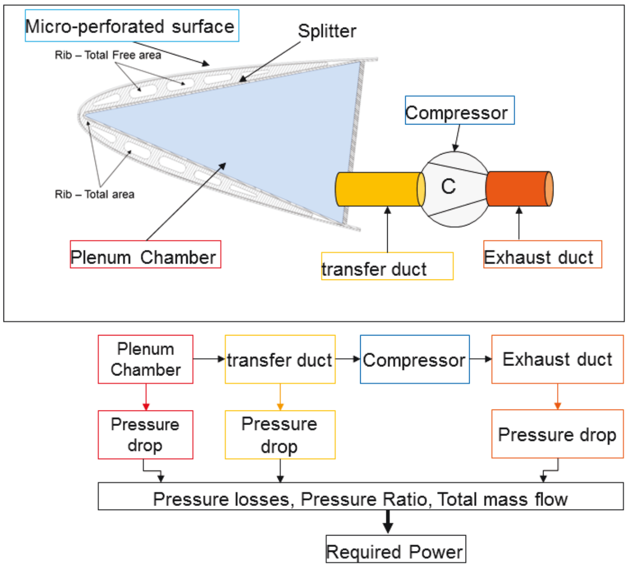

FIG 8. Schematic explaining various pressure losses

(1) $$\Delta p_{contra} = \frac{\rho}{2} v_1^2 * 0.5 * \left(1 - \frac{F_1}{F_0}\right)^{3/4}$$

where ρ is the density of air in the plenum, *v* is the velocity, F_1, F_0 are cross sectional areas. The indices 1 and 0 represent conditions after and before contraction, respectively.
The pressure losses in the ducts [11, 12] can be calculated using Eqn. 2

(2) $$\Delta p_{duct} = \delta_{duct} \rho \frac{v^2}{2} = \lambda_{duct} \frac{L}{D_h} \rho \frac{v^2}{2}$$

where δ_{duct} is the resistance coefficient, λ_{duct} is the pipe friction coefficient, D_h is the hydraulic diameter, *v* is the flow velocity through the pipe.
Once the pressure losses on both the upstream and downstream side of the compressor are calculated, the pressure at the compressor inlet (P_{in}) and outlet (P_{out}) and hence the pressure ratio (*PR*) can be determined.

(3) $$PR = \frac{P_{out}}{P_{in}}$$

For the calculated pressure ratio and known mass flow ($\dot{m}$), the isentropic suction power can be estimated as given by Eqn. 4

(4) $$P_{is\_suction} = \dot{m}\left(\frac{\gamma}{\gamma-1}\right) R T_{duct}\left[(PR)^{\left(\frac{\gamma-1}{\gamma}\right)} - 1\right]$$

where γ is the ratio of specific heats with value 1.4 for dry air, T_{duct} is the temperature in the plenum and *R* = 287.15 J/kg/K is the universal gas constant.

The shaft / compressor power and electrical / drive power can be determined as given in Eqns. 5 and 6, respectively.

(5) $$P_{compressor} = \frac{P_{is\_suction}}{\eta_{compressor}}$$

(6) $$P_{drive} = \frac{P_{compressor}}{\eta_{drive}}$$

Finally, the power off-take (POT) from the engine generator for the HLFC system can be calculated as per Eqn. 7.

(7) $$POT = \frac{P_{drive}}{\eta_{gen}\eta_{pl}}$$

where $\eta_{compressor}$, η_{drive}, η_{gen}, η_{pl} are the efficiencies of compressor, drive, engine generator and power line, respectively.
The additional fuel flow due to HLFC system POT can be calculated using Eqn. 8 [13]

(8) $$\dot{m}_{F,HLFC} = k_p * SFC * POT$$

where k_p is the shaft power factor and has a value of 0.00182 N/W for the CFM56 engines [13] of the reference aircraft, SFC is their specific fuel consumption which is approximately 16 g/kN/ s. The nominal SFC change due to the HLFC system can be calculated for a given thrust *T* as follows

(9) $$\Delta SFC_{HLFC} = \dot{m}_{F,HLFC} / T$$

3.2. System mass estimation

The total HLFC system mass can be calculated as the sum of electrical equipment mass, ducting mass, added structural mass and compressor mass.

(10) $$m_{HLFC\_system} = m_{electrical} + m_{ducting} + m_{structure} + m_{compressor}$$

The electrical mass (Eqn. 11) is due to the electrical wires and other additional equipment (power supply unit / inverters). The mass of wires can be calculated using the values of mass per unit length of the (standard) wire (m'), length of wire from power generation till suction area (l) and the total electrical power required

(11) $$m_{electrical} = m_{wires} + m_{equipment}$$

(12) $$m_{wires} = m' * l * P_{drive}$$

The mass of the ducting can be estimated if the material density, cross-sectional area and length of the duct are known as given by Eqn. (13). The ducting is designed so as to limit the exhaust flow velocity to a Mach number of 0.2.

(13) $$m_{ducting} = A_{duct} * l_{duct} * \rho_{duct}$$

Instead of empirical estimation as in [14], the design and mass of the electric air compressor is estimated using an in-house tool. The design and selection of the compressor is made with the help of a Cordier diagram [15] so as to satisfy the given space constraints. The optimal compressor for the investigated architectures was found to be a radial compressor coupled with an induction motor (drive). Its mass can be estimated as given in Eqn. 14.

(14) $$m_{compressor} = m_{impeller} + m_{casing} + m_{drive}$$

where $m_{impeller}$, m_{casing}, m_{drive} are the mass of impeller, casing for the compressor, and drive, respectively.

The structures discipline provided the additional structural mass added due to the HLFC system. It includes mass of the newly added micro-perforated surface, the splitter section and the ribs. The total leading edge structural mass is compared to that of a normal A320 aircraft, and the difference is used in the added structural mass calculations.

4. SYSTEM ARCHITECTURES STUDY

In order to attain the said benefits of the HLFC system, the optimal system architecture needs to be identified for further development and detailed design. In the preliminary phase, several possible architectures are defined and assessed to check for feasibility, added mass and power consumption.

4.1. HLFC system architectures definition

Fig. 9 shows the various proposed architectures for the chamberless active HLFC system for the VTP. The length of the electrical wires is assumed to be the distance between the electrical and electronics bay (E/E bay) and the compressor location at the VTP. In Architectures 1 to 3, only one compressor is employed to achieve the suction requirements. The pneumatic duct in green colour indicates the transfer duct from the plenum to the compressor inlet. The exhaust duct from the compressor outlet to the exhaust valve is marked in orange colour.

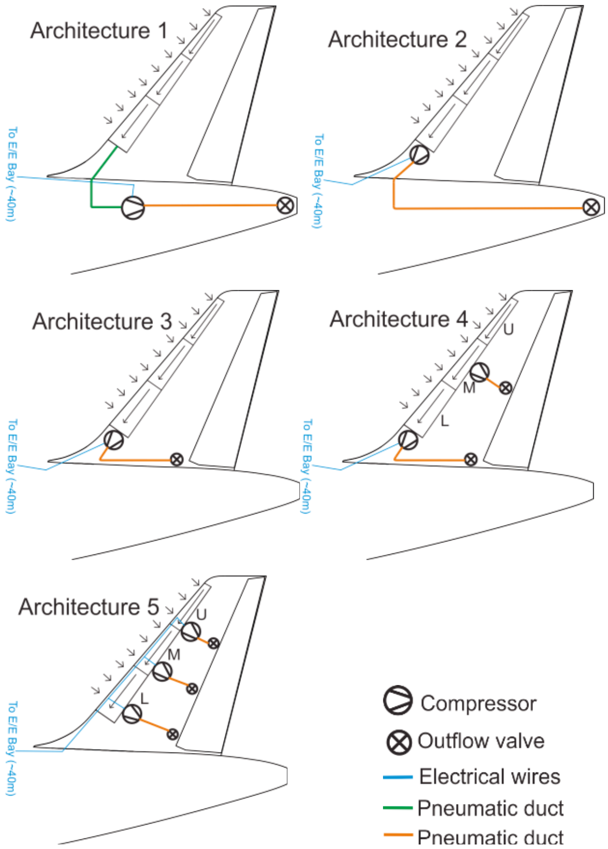

FIG 9. Investigated HLFC system architectures for VTP

The transfer duct is present only in architecture 1. In architectures 2 and 3, the compressor is directly connected to the plenum chamber and the positions of the exhaust valves are varied. Architecture 4 has two compressors, where the first compressor is exclusively provided for the lower segment L and the second compressor for the combined middle (M) and upper (U) segments with a separate exhaust. In architecture 5, each segment is provided with a separate compressor with an individual outlet.

4.2. Architecture assessment and comparison

For the proposed architectures (Arch), the suction power requirements, the power off-takes, the total system mass, and the additional fuel flow due to the HLFC system are calculated using the method explained in section 3. The results are summarized in Table 1.

Arch	Pump power (kW)	Drive power (kW)	POT (kW)	HLFC system mass (kg)	Additional fuel mass flow due to HLFC system (g/s)
1	13.2	15.0	20.6	69.5	0.60
2	12.5	14.0	19.5	69.0	0.57
3	12.3	13.6	19.0	55.4	0.55
4	12.2	13.6	19.0	60.0	0.55
5	11.8	13.2	18.5	55.0	0.54

TAB 1. Comparison of VTP HLFC Architectures

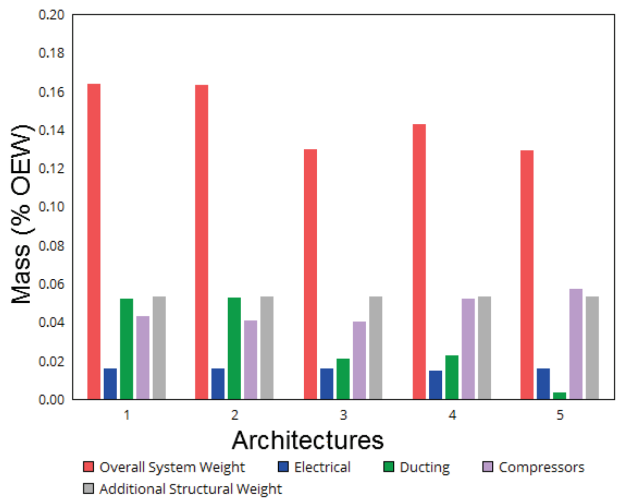

FIG 10. HLFC system mass breakdown for different architectures in terms of percentage OEW

In Fig. 10, the HLFC system mass breakdown is shown as percentage of the overall empty weight (OEW) of an A320 aircraft (WV 003, 42300 kg [with CFM engines]). It becomes evident that much of the weight contribution is due to ducting and compressors. This can be seen in architectures 1 and 2. Adding more compressors increases the overall weight in multi-compressor architectures such as architectures 4 and 5. The reduction in ducting length, however, in general helps in reducing overall system weight.

The calculations for all the above architectures are performed for the design point, which was set at FL 310 (31000 ft). The HLFC system is intended to operate between FL290 and the service ceiling at FL400 feet. Hence, it is interesting to evaluate the performance for off-design conditions as well. Exemplarily architecture 1 is selected to compare the performance at different flight altitudes. The calculations are shown in Appendix A, the obtained results plotted in Figs. 11 and 12.

Fig. 11 shows the variation in compressor power with altitude for an exhaust flow Mach number of 0.2. The compressor power requirement is a function of pressure ratio, pressure losses and mass flow as shown in Eqn. 4 and all these three quantities change with altitude. Consequently the suction power needed to produce the plenum pressure is highly dependent on the flight level. An increase in flight level results in lower suction power requirements, as air density and mass flow requirements are decreased. A similar trend is followed for the compressor design point: Fig. 12 shows how the compressor mass varies with different design flight levels (FL310 being the reference). The optimal altitude should be chosen so as to have a compromise between good aerodynamic performance and optimal system mass and power costs.

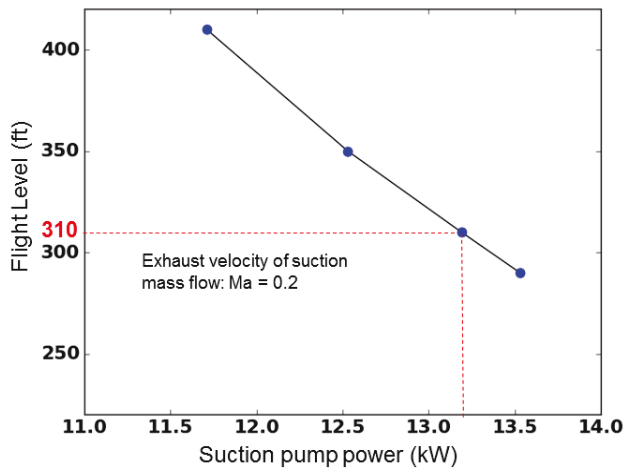

FIG 11. Variation of compressor power with different flight levels

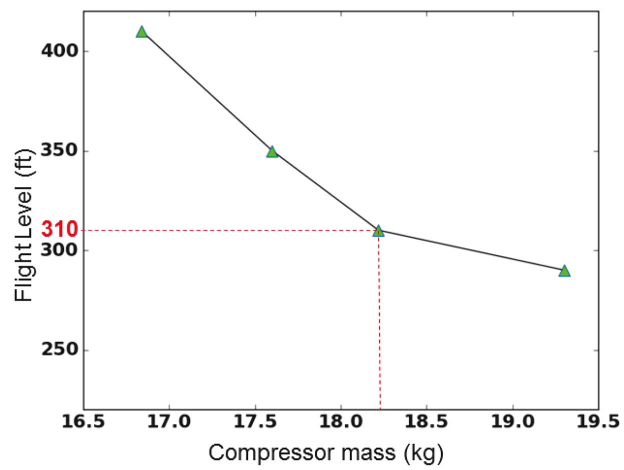

FIG 12. Variation of compressor mass with different flight levels

4.3. Discussion of results

Table 1 indicates that architectures 1 and 2 have very high system masses and relatively high power off-takes due to heavy pressure losses in the long ducts. In terms of total system mass and power off-take architectures 3 and 5 are the best. The SFC change is approximately 0.03% for all the architectures.

In this investigation, the redundancy aspect is not considered. Adding redundancy by providing a back-up compressor adds more reliability, but will also add more system weight. It is also necessary to investigate whether a back-up compressor can be installed with the given space constraints. The aircraft installed with the HLFC system is expected to consume less fuel than without, and hence carries less fuel to minimize weight. In the event of a total failure of the HLFC system, contingency measures may be necessary to avoid fuel depletion, depending on the particular operation, flight plan and available fuel to destination without a functioning HLFC system. The cockpit crew should be alerted if the system fails and the range reduction without HLFC system should be made available.

Note that in architecture 3 there will be a complete loss of laminarity if the compressor fails, while in architecture 5, partial laminarity will still exist with a single compressor failure, since different compressors operate on different segments.

On the other hand, in terms of integration aspects and maintenance, architecture 5 adds complexity and has to be further scrutinized by doing mock-up studies for architectural feasibility and system maintainability. Also, in architecture 5, the compressors are placed behind the front spar. The hot exhaust air from the compressor might create humidity problems eventually leading to fungus production in that area. So anti-bacterial painting of the whole area is necessary to avoid this problem, necessitating further maintenance effort for architecture 5.

In addition to the key parameters mentioned in the paper, a qualitative comparison is made with five criteria as shown in Table 3, and the relative optimal architecture is found to be architecture 3.

Criteria	Total Score	Architecture 3	Architecture 5
Power consumption	4	4	4
System mass	4	4	4
Total loss of laminarity	4	1	4
Feasibility	4	4	2
Maintainability	4	4	1
Relative optimal architecture	20	17	15

TAB 2. Qualitative assessment between architectures

5. CONCLUSION AND OUTLOOK

This paper analyzed a potential chamberless active HLFC system for a mid-range aircraft. The method for system assessment was explained along with the key parameters for optimal architecture selection. Various system architectures were proposed and assessed. A comparison of architectures was performed with key parameters such as system mass, power consumption and specific fuel consumption to do trade-off study. The system performance was also evaluated for off-design conditions. The optimal altitude for HLFC system operation is a trade-off between aerodynamic performance and system mass and power costs.

A digital mock-up study is suggested for further investigation of the proposed architectures, which helps in assessing the feasibility in detail. Such an architecture selection process during the preliminary design phase helps in cost-cutting and selection of optimal architecture for detailed design.

The HLFC system is a multi-disciplinary and complex system and problems with hazards such as contamination, icing and rain still exist. These effects could potentially clog the micro-perforated surface and bring down the effectiveness of the system. The selected optimal suction system architecture as explained in the paper has to be complemented with additional sub-systems to protect the system from these potential hazards. These sub-systems add complexity, and an optimal solution needs to be chosen in order to obtain the said benefits. So the optimal HLFC system is a combination of optimized suction system architecture along with the optimal system solution for hazard protection, and it needs to be shown at aircraft level that the obtainable fuel savings outweigh the weight, maintenance and production cost penalties of the system.

6. REFERENCES

[1] Green E. John, “Laminar Flow Control - Back to the Future?”, AIAA 2008-3738.

[2] K.S.G. Krishnan, O. Bertram and O. Seibel, 2017, “Review of Hybrid Laminar Flow Control Systems”, *Progress in Aerospace Sciences*.

[3] R. D. Joslin; 1998; "Overview of Laminar Flow Control"; *NASA/TP-1998-208705;* Hampton, VA; USA

[4] T. Pe, F. Thielecke, 2010, Methodik zur Leistungsabschätzung von HLFC-Absaugsystemen im Flugzeugvorentwurf, 2010. Deutscher Luft- und Raumfahrtkongress.

[5] G.H. Schrauf, 2005, “Status and perspectives of laminar flow”, *Aeronautical J. 109 (2005).*

[6] K. Risse, et al., Conceptual wing design methodology for aircraft with hybrid laminar flow control, in: 52nd Aerospace Sciences Meeting Held at the AIAA SciTech Forum, Maryland, 2014.

[7] J.-P. Robert, “Drag Reduction: an Industrial Challenge”, *AGARD Special Course on Skin Friction Drag Reduction, 1992*. AGARD-R-796

[8] NASA-CR-1999–209326, High Reynolds Number Hybrid Laminar Flow Control (HLFC) Flight Experiment IV – Suction System Design and Manufacture, 1999.

[9] G. Schrauf, K.H. Horstmann; 2004; "Simplified Hybrid Laminar Flow Control"; *European Congress on Computational Methods om Applied Sciences and Engineering;* Jyväskylä, Finland

[10] M. Horn, A. Seitze, M. Schneider; “Novel Tailored Skin Single Duct Concept for HLFC Fin Application“, 7th European Conference for Aeronautics and Space Sciences (EUCASS), 2015

[11] I.E. Idelchik; 1994; "Handbook of hydraulic resistance"; *3rd ed., CRC Press Boca Raton*

[12] T. Pe, F. Thielecke; "Synthesis and Topology Study of HLFC System Architectures in Preliminary Aircraft Design"; 3rd *CEAS Air & Space Conference;* Venice; Italy; pp. 1460-1471, 2011

[13] D. Scholz., “Fuel consumption due to shaft power off takes from the engine”, *Aircraft Systems Technology Conference 2013*, Hamburg, Germany

[14] M. Jabbal , S. Everett, K.S.G. Krishnan, S. Raghu, "A Comparative Study of Hybrid Flow Control System Architectures for an A320 Aircraft, 8th AIAA Flow Control Conference, AIAA AVIATION Forum, (AIAA 2016-3928). Washington D.C.

[15] O. Cordier, “Ähnlichkeitsbedingungen für Strömungsmaschinen”, Brennstoff, Wärme, Kraft (BWK), Vol. 5, No. 10, 1953, pp. 337-340”

APPENDIX A

		Off-Design	Design Point	Off-Design	Off-Design
Flight level (ft)		29000	31000	35000	40000
Parameters					
Standard Atmosphere	P_0 (Pa)	31485	28745	23842.3	18753.9
	T_0 (K)	230.7	226.7	218.8	216.7
	ρ_0 (kg/m³)	0.47544	0.44165	0.37960	0.30156
Condition at Vertical Tail Plane	P_∞ (Pa)	31480	28741	23839	18708
	T_{in} (K)	252	247	239	230
	P_{plenum} (Pa)	25740	23000	18097.3	13008.9
	P_{inlet} (Pa)	25158.2	22482.5	17693.6	12721.6
	ρ_{plenum} (kg/m³)	0.35590.	0.32445	0.26384	0.19707
Suction compressor design data for M = 0.2	mass flow (kg/s)	0.520	0.474	0.385	0.288
	$\dot{V}_{in}$ (m³/s)	1.461	1.461	1.461	1.461
	P_{outlet} (Pa)	32086.5	29292.5	24292.4	19107.1
	PR (-)	1.275	1.303	1.373	1.502
Isentropic power	P_{is} (kW)	9.47	9.23	8.77	8.20
Compressor Shaft power	P_{shaft} (kW)	13.53	13.19	12.53	11.71
Drive electric power	$P_{electric}$ (kW)	15.04	14.66	13.92	13.01